

Supplemental Material

Gate-tuned two-channel Kondo screening by graphene leads: Universal scaling of the nonlinear conductance

Tsung-Han Lee¹, Kenneth Yi-Jieh Zhang¹, Chung-Hou Chung^{1,2}, Stefan Kirchner^{3,4}

¹*Department of Electrophysics, National Chiao-Tung University, HsinChu, Taiwan, 300, R.O.C.*

²*National Center for Theoretical Sciences, HsinChu, Taiwan, 300, R.O.C.*

³*Max-Planck-Institut für Physik komplexer Systeme, 01187 Dresden, Germany*

⁴*Max-Planck-Institut für chemische Physik fester Stoffe, 01187 Dresden, Germany*

PACS numbers:

A: NON-EQUILIBRIUM NCA

The extension of the non-crossing approximation onto the Keldysh contour has been discussed in several papers [1, 2]. It is customary to neglect the bias voltage dependence of the conduction electron density of states (DOS) $\rho(\epsilon)$. This is justified provided ρ is well approximated by a constant in a region around the Fermi energy that is large compared to the applied bias voltage. When the DOS vanishes in a power-law fashion at or near the Fermi energy, this is no longer possible and the equations have to be generalized appropriately. The full set of equations to be solved for the two-channel pseudogap problem becomes

$$\begin{aligned}\Sigma_B^<(\omega) &= (-2i) \int_{-\infty}^{\infty} d\epsilon G_f^<(\epsilon + \omega) \left[|V_L|^2 f(-\epsilon + \mu_L) \times \right. \\ &\quad \left. \rho_L(\epsilon - \mu_L - \mu) + |V_R|^2 f(-\epsilon + \mu_R) \rho_R(\epsilon - \mu_R - \mu) \right] \\ \Sigma_B^>(\omega) &= 2i \int_{-\infty}^{\infty} d\epsilon G_f^>(\epsilon + \omega) \left[|V_L|^2 f(\epsilon - \mu_L) \times \right. \\ &\quad \left. \rho_L(\epsilon - \mu_L - \mu) + |V_R|^2 f(\epsilon - \mu_R) \rho_R(\epsilon - \mu_R - \mu) \right]\end{aligned}$$

for the pseudo-boson and

$$\begin{aligned}\Sigma_f^<(\omega) &= 2i \int_{-\infty}^{\infty} d\epsilon G_B^<(\epsilon + \omega) \left[|V_L|^2 f(-\epsilon + \mu_L) \times \right. \\ &\quad \left. \rho_L(-\epsilon + \mu_L + \mu) + |V_R|^2 f(-\epsilon + \mu_R) \rho_R(-\epsilon + \mu_R + \mu) \right] \\ \Sigma_f^>(\omega) &= 2i \int_{-\infty}^{\infty} d\epsilon G_B^>(\epsilon + \omega) \left[|V_L|^2 f(\epsilon - \mu_L) \times \right. \\ &\quad \left. \rho_L(-\epsilon + \mu_L + \mu) + |V_R|^2 f(\epsilon - \mu_R) \rho_R(-\epsilon + \mu_R + \mu) \right]\end{aligned}$$

for the pseudo-fermion. The DOS (ρ_L and ρ_R) of the two leads do not have to be identical. The bias voltage applied across the system is $eV^{\text{bias}} = \mu_L - \mu_R$, where μ_L and μ_R are the chemical potentials of the left and right leads.

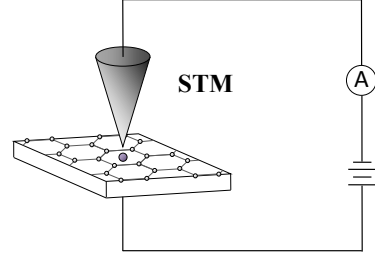


FIG. 1: The STM measurement of the magnetic adatom in graphene. The $S = 1/2$ magnetic adatom is located at the center of the honeycomb lattice of graphene.

B: FANO-LINESHAPES

An experiment reminiscent of the situation considered by us has been performed recently, where magnetic adatoms on graphene were investigated via scanning tunneling microscopy (STM), see Ref. 7. Our analysis can be extended to include the current-voltage characteristics measured by an STM (see Fig.1). In this case, one of the two fermionic leads represents the STM tip and it is necessary to explicitly allow for the different tunneling paths between the STM tip, the adatom and the substrate which will act as the second lead. An important difference between the STM setup and our analysis so far is that the STM tip is a *good* metal, *e.g.* a single-channel lead with constant DOS at its Fermi energy. We here will model it by a two-channel lead with constant DOS at its Fermi energy. This is justified provided the coupling between the STM tip and the system is small as the RG scaling equations for two and one-channel case are identical up to fourth order in the tunneling matrix element.

The theory of STM on magnetic adatoms on a metal surface has been worked out by Schiller and Hershfield [3] and by O. Újsághy et al. [4]. The current is obtained from

$$I(V) \sim \int_{-\infty}^{\infty} d\epsilon \left[f(\epsilon - eV^{\text{bias}}) - f(\epsilon) \right] \rho_{\text{tip}} \rho_{\text{eff}}(\epsilon), \quad (1)$$

where ρ_{tip} is the density of states of the STM tip and ρ_{eff} is an effective density of states probed by the STM and

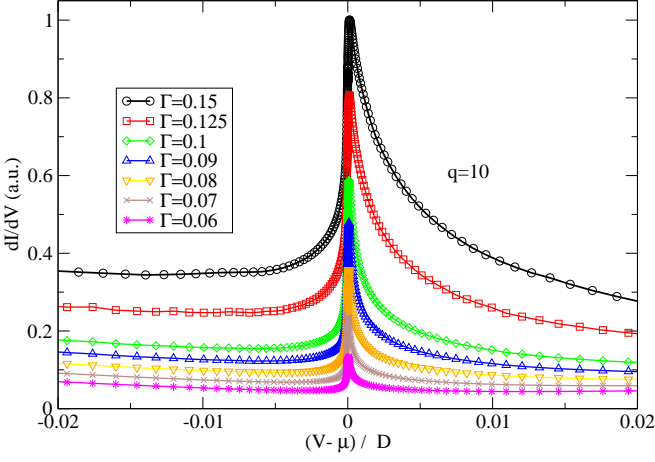


FIG. 2: Fano-lineshapes with Fano parameter $q = 10$ for various values of Γ (in units of the half-bandwidth D). Here, we have set $\epsilon_d = -0.2D$, $\mu = -0.1D$.

depends on two tunneling rates t_f and t_c that parameterize the hybridization strength of the STM tip with the magnetic adatom (t_f) and the graphene leads (t_c). The effective density of states ρ_{eff} can be recast into

$$\rho_{\text{eff}} = \frac{1}{\pi} \text{Im} \left[t_c^2 G_c(\vec{R}, \vec{R}, \epsilon) + (t_d + t_c V G_c(\vec{R}, \vec{R}_{ad}, \epsilon)) \times G_{ad}(\epsilon) (t_d + t_c V^* G_c(\vec{R}_{ad}, \vec{R}, \epsilon)) \right], \quad (2)$$

where V is the hybridization strength between the graphene electrons and the magnetic adatom, $G_c(\epsilon)$ is the advanced local graphene electron Green function at the locus of the STM tip \vec{R} and $G_c(\vec{R}, \vec{R}_{ad}, \epsilon)$ is the advanced graphene electron Green function connecting the locus of the tip with the position of the adatom at \vec{R}_{ad} , and t_c (t_d) is the tunneling matrix element between the STM tip and the substrate (magnetic adatom). $G_{ad}(\epsilon)$ is the advanced Green function of the magnetic adatom that can be obtained from the pseudo-particle Green functions of section A.

In the linear regime, the Fano lineshape is given by the differential conductance $dI/dV|_{V \rightarrow 0}$, which turns out to be proportional to the effective density of states $\rho_{\text{eff}}(\epsilon)$: $dI/dV|_{V \rightarrow 0} \propto \rho_{\text{eff}}(\epsilon = V)$.

$dI/dV|_{V \rightarrow 0}$ can be cast into the Fano lineshape where the Fano parameter q is given by [4–6]

$$q = -\frac{\text{Re} G_c^0(\epsilon - i\eta)}{\text{Im} G_c^0(\epsilon - i\eta)}, \quad (3)$$

and can be treated as approximately constant in the energy range of interest [5].

Typical Fano-lineshapes in the linear regime are shown in Fig. 2. The 2CK behavior seen in the STM measurement [7] for Co-adatom at the center of the honeycomb lattice is signaled by the Kondo peaks at $\omega = \mu$ in Fano-

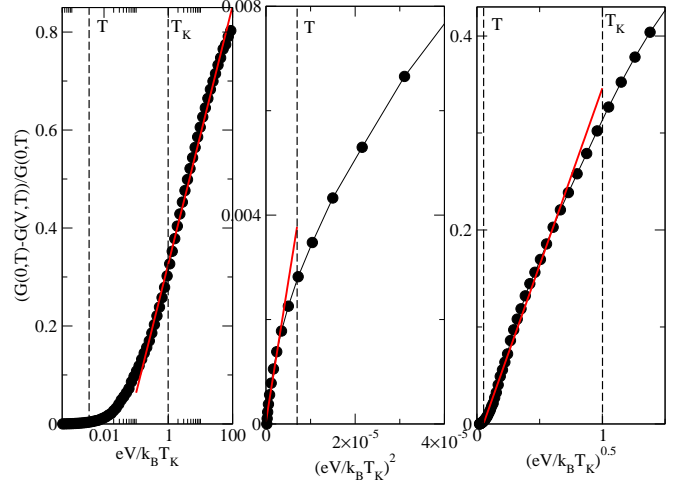


FIG. 3: Non-linear conductance for a large $\Gamma = 0.1D$ between impurity and graphene substrate and a much smaller hopping Γ_{ts} between tip and the impurity, $\Gamma_{st} \ll \Gamma$, corresponding to the STM measurement reported in [7]. The $G(V, T)$ curves agree well with the STM results of [7]. (a) $\log V$ dependence around $V \sim T_K$. (b) V^2 behavior for $V < T$. (c) $T^{1/2}$ 2CK behavior for $T < V < T_K$. Here, $T = 5 \times 10^{-7}D$. The other parameters are: $\mu = -0.1D$, $\epsilon_d = -0.2D$.

lineshapes, which are compatible with a large fitting parameter q (for example $q = 10$) and a correspondingly small t_c/t_d and concomitantly small intervalley scattering.

C. UNIVERSAL 2CK-LM CROSSOVER FOR $\mu > 0$

In the main text, we focus on the universal 2CK-LM crossover for negative chemical potential, $\mu < 0$. A similar scaling behaviors can also be found in conductance for positive μ . As shown in Fig. 4, for a fixed positive $\mu = 0.1D$, the linear conductance $G(T)$ vs. hybridization Γ follows a single universal scaling form of T/T^* . The single scaling form of $G(T)$ we observe here for $\mu > 0$ is somewhat surprising as for $\mu < 0$ the conductance shows two distinct scaling regimes: $T < T_K$ and $T > T^*$. We believe that this difference maybe due to the particle-hole asymmetry in our model as the Kondo peak, located at $\omega = \mu$, is affected more by the charge peak at $\epsilon_d < 0$. for $\mu < 0$ than that for $\mu > 0$.

Similar to the case for $\mu < 0$, the linear conductance for $\mu > 0$ shows a typical 2CK \sqrt{T} behavior for $T < T_K$, and a universal power-law behavior at high temperatures for $\Gamma \rightarrow \Gamma^*$: $G(T) \propto (T/T^*)^\alpha$ with $\alpha \approx 0.00009 \approx 0$. The Kondo temperature T_K and the crossover scale T^* for $\mu > 0$ behave in a similar way to their $\mu < 0$ counterparts: $T_K \propto \Gamma \times e^{-1/\Gamma}$, $T^* \propto (\Gamma - \Gamma^*)^{1/\nu}$ with $\Gamma^* \approx 0.06D$ and $\nu \sim 0.05$. We believe that our results for both posi-

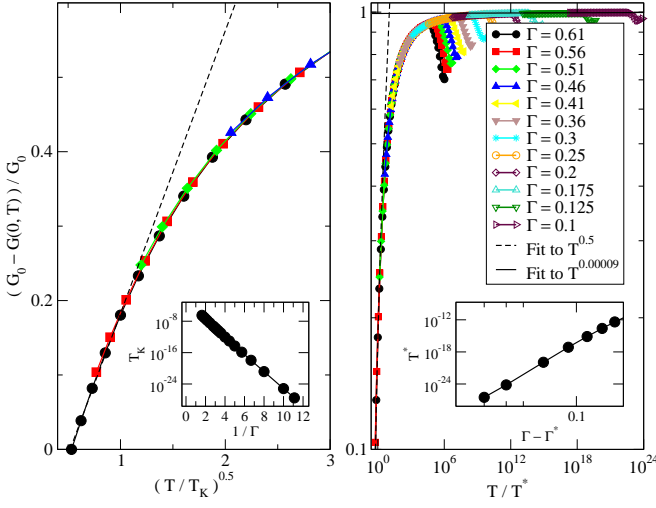


FIG. 4: Universal scaling in linear conductance $G(T)$ as a function of temperature T for at fixed positive chemical potential $\mu = 0.1D$ and for various values of hybridization Γ . (a) $T^{1/2}$ 2CK behavior for $T < T_K$ for large values of Γ . Inset: T_K/Γ vs. $1/\Gamma$. (b) Universal scaling of $G(T)$ for smaller values of Γ . Inset: The crossover energy scale T^* as a power-law function of $\Gamma - \Gamma^*$. Here, $\epsilon_d = -0.2D$, G_0 is the linear conductance for $\Gamma = 0.62D$ at $T = 5 \times 10^{-7}D$, and $\Gamma^* \approx 0.06D$.

tive and negative values of μ could be used as theoretical guidance in future experiments to clarify the issue on two-channel Kondo physics in graphene.

-
- [1] Matthias H. Hettler, Johann Kroha, and Selman Hershfield, Phys. Rev. Lett. **73**, 1967 (1994); Ch. Kolf, J. Kroha, M. Ternes, and W.-D. Schneider, Phys. Rev. Lett. **58**, 5649 (1998).
 - [2] Ned S. Wingreen and Y. Meir, Phys. Rev. B **49**, 11040 (1994).
 - [3] A. Schiller and S. Hershfield, Phys. Rev. B **61**, 9036 (2000).
 - [4] O. Újsághy et al. Phys. Rev. Lett. **85**, 2557 (2000).
 - [5] U. Fano, Phys. Rev. **124**, 18661878 (1961).
 - [6] Chung-Hou Chung and Tsung-Han Lee, Phys. Rev. B **82**, 085325 (2010).
 - [7] L. S. Mattos *et al.*, (un-published).
 - [8] V. Madhavan, W. Chen, T. Jamneala, M. F. Crommie, and N. S. Wingreen, Phys. Rev. B **64**, 165412 (2001).

Gate-tuned two-channel Kondo screening by graphene leads: Universal scaling of the nonlinear conductance

Tsung-Han Lee¹, Kenneth Yi-Jieh Zhang¹, Chung-Hou Chung^{1,2}, Stefan Kirchner^{3,4}
¹*Electrophysics Department, National Chiao-Tung University, HsinChu, Taiwan, 300, R.O.C.*
²*National Center for Theoretical Sciences, HsinChu, Taiwan, 300, R.O.C.*
³*Max-Planck-Institut für Physik komplexer Systeme, 01187 Dresden, Germany*
⁴*Max-Planck-Institut für chemische Physik fester Stoffe, 01187 Dresden, Germany*
(Dated: February 20, 2013)

Based on the non-crossing approximation, we calculate both the linear and nonlinear conductance within the two-lead two-channel single-impurity Anderson model where the conduction electron density of states vanishes in a power-law fashion $\propto |\omega - \mu_F|^r$ with $r = 1$ near the Fermi energy, appropriate for an hexagonal system. For given gate voltage, we address the universal crossover from a two-channel Kondo phase, argued to occur in doped graphene, to an unscreened local moment phase. We extract universal scaling functions in conductance governing charge transfer through the two-channel pseudogap Kondo impurity and discuss our results in the context of a recent scanning tunneling spectroscopy experiment on Co-doped graphene.

PACS numbers:

Introduction. The two-channel Kondo [1] (2CK) problem [2] is a fascinating example of an exotic quantum many-body phenomenon resulting in a metallic ground state with non-Fermi-liquid behavior. It involves a single quantum impurity spin with $s = 1/2$ that couples antiferromagnetically to two identical conduction electron reservoirs. As a result, Kondo processes involving both reservoirs lead to overscreening of the local moment. Theoretically, the 2CK physics has been studied extensively via Bethe ansatz [3], conformal field theory [4], bosonization [5] and the numerical renormalization group [6]. Experimentally, however, up to date, only very few examples of clear 2CK physics have been experimentally realized, *e.g.* in semiconductor quantum dots [7], in magnetically doped nanowires, and in metallic glasses [8, 9].

Recently, the Kondo effect of magnetic adatoms in graphene has attracted much attention, theoretically [10, 11] as well as experimentally [12] due to the possible realization of a 2CK ground state. One interesting aspect of Kondo physics in graphene is due to the Dirac (linear) spectrum that gives raise to a pseudogap local density of states (DOS), $\rho_c(\omega) \propto |\omega|^r$ with $r = 1$, at the impurity site, making graphene one of the few experimental realizations of the pseudogap Kondo model [13, 14], the simplest model to study critical Kondo destruction [15, 16]. In the pseudogap Kondo (or more generally Anderson) model, a quantum phase transition is expected between the Kondo screened and the unscreened local moment (LM) ground states for $0 < r < 1$ [14, 17]. For $r = 1$, the case of graphene, Kondo screening does not occur [11, 14, 20], resulting in a LM ground state. Yet, Kondo screening can be induced by changing the Fermi energy, *e.g.* by applying a gate voltage ($\mu \neq 0$).

That two independent screening channels can exist in graphene is related to the existence of two inequivalent Dirac points (K and K') in its band structure. It therefore was argued that the effective low-energy model for

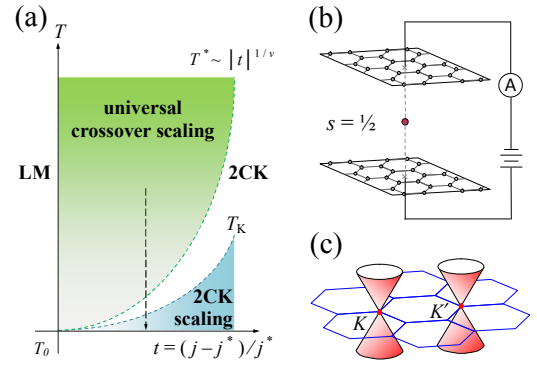


FIG. 1: (a) Schematic phase diagram for the 2CK-LM crossover. The parameter j refers to either Γ or μ (in units of $D = 1$), and j^* refers to the crossover scale for a fixed temperature $T_0 \sim 5 \times 10^{-7} D$. T_K and T^* represent crossover energy scales associated with the universal scaling for 2CK (blue shaded) and the high-temperature 2CK-LM crossover scaling (green shaded) regime, respectively. (b) Schematic setup of the model in Eq. (1): a $S = 1/2$ impurity (red dot) couples symmetrically to the two sub-lattices of two graphene leads that are kept at different chemical potentials of the setup. (c) Dirac points (labeled by K and K') with its Dirac spectrum on graphene's honeycomb lattice in momentum space.

magnetic impurities in graphene depends on the location of the adatom [21]: if the impurity is located at the center of the cell, the inter-valley scattering does not couple the two screening channels and an effective 2CK ensues [10]. This has been explicitly demonstrated within a tight-binding description where the hybridization between electronic states in graphene and impurity states preserves the A-B sub-lattice symmetry [22]. The situation is different if the adatom is located on a graphene site and the sub-lattice symmetry is absent in the impurity-graphene hybridization. The effective low-energy model is in this case the more conventional one-

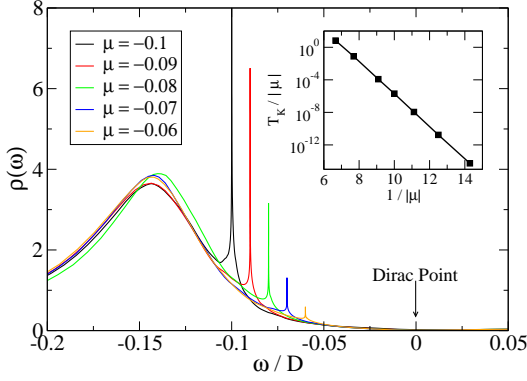


FIG. 2: The impurity spectral function $\rho(\omega)$ vs. chemical potential μ (in units of the bandwidth D). The Kondo peak is pinned near μ . The Dirac point is assigned $\omega = 0$. Inset: Kondo temperature T_K (defined in text) as a function of μ . The NCA parameters are $T = 5 \times 10^{-7}D$, $\Gamma = 0.2D$, $\epsilon_d = -0.2D$.

channel pseudogap Kondo model [21, 22]. The difference between the various adatom positions can be probed by scanning tunneling microscopy (STM) [23, 24]. This has been achieved recently with *Co*-atoms as magnetic adatoms where signatures of 2CK physics are seen when the adatom is located at the zone center of the honeycomb cell such that the inter-valley scatterings between K and K' Dirac electrons are strongly suppressed [12].

The 2CK-LM quantum phase transition in the two-channel pseudogap Kondo and Anderson model with $\mu = 0$ and $0 < r < 1$ in and out of equilibrium has been studied recently [14, 18–20], but the experimentally more relevant situation of $r = 1$ and $\mu \neq 0$ has not yet been properly addressed. The possibility of realizing 2CK physics was first pointed out in Ref. [10]. There is, however, a lack of systematic investigations beyond the mean-field treatment. In this letter, we study the crossover phenomenon from the LM to 2CK regime, and work out the universal scaling functions of the conductance. A comprehensive analysis of the non-equilibrium transport, including STM lineshapes in the various regimes is presented. We address this issue using the non-crossing approximation (NCA) [25–27], which is known to give reliable results for multi-channel Kondo systems which are in line with conformal field theory results [8]. It has been shown recently that the NCA is able to reproduce the correct qualitative features of the two-channel pseudogap model for $0 \leq r \leq 1$ in and out of equilibrium in excellent agreement with exact results [18, 19].

Here, we study the steady-state transport properties of the experimentally most relevant pseudogap case, $r = 1$ as a function of doping, temperature and bias voltage.

The Model Hamiltonian. Our starting point is the two-lead two-channel single-impurity pseudogap Ander-

son model. Each lead is characterized by a power law density of states (DOS) ($\rho_c(\omega) \sim |\omega|\Theta(D-|\omega|)$, where D is a high-energy cutoff that serves as our unit of energy $D = 1$). A possible realization of this model is sketched in Fig. 1 (b) where a spin-1/2 impurity is coupled to two graphene leads with couplings to each lead preserving the sub-lattice symmetry of the honeycomb lattice [12, 22].

Within a pseudofermion representation, the Hamiltonian reads [26, 27]

$$H = \sum_{k,\sigma,\tau,\alpha} (\epsilon_k - \mu_\alpha) c_{k\sigma\tau}^\dagger c_{k\sigma\tau}^\alpha + \epsilon_d \sum_\sigma f_\sigma^\dagger f_\sigma + \sum_{k,\sigma,\tau,\alpha} (U_\alpha (f_\sigma^\dagger b_\tau c_{k,\sigma,\tau}^\alpha) + \text{h.c.}), \quad (1)$$

where μ_α is the chemical potential of lead α , and $\alpha = L/R$ labels the two conduction electron leads. The indices σ and τ refer to spin and charge (related to K and K') channels characterizing the conduction electrons. The second and third term of the RHS of Eq. (1) represent the spin-1/2 and the hybridization strength U_α between the graphene electrons and the impurity. In the pseudofermion representation the local electron is decomposed as $d_{\sigma,\tau}^\dagger = f_\sigma^\dagger b_\tau$. Eq. (1) is a faithful representation of the two-channel single-impurity pseudogap Anderson model, provided the constraint $Q = \sum_\sigma f_\sigma^\dagger f_\sigma + \sum_\tau b_\tau^\dagger b_\tau = 1$ is fulfilled at all times. A finite bias voltage is implemented by shifting the chemical potentials in the leads such that $\mu_L - \mu_R = eV$ is the applied bias voltage across the 2CK system [24].

To study the properties of Eq. (1) we employ the NCA. Its ability to correctly capture the properties of the pseudogap two-channel Anderson model was established recently [18, 19]. Within the NCA, the retarded self-energy for pseudofermions, $G^r(\omega) = [\omega - \epsilon_d - \Sigma^r(\omega)]^{-1}$, and slave-bosons, $D^r(\omega) = [\omega - \Pi^r(\omega)]^{-1}$, are [18, 19, 26, 27]

$$\Sigma^r(\omega) = \frac{2}{\pi} \sum_\alpha \int d\epsilon \Gamma_\alpha(\omega - \epsilon - \mu_\alpha) f(\epsilon - \omega - \mu_\alpha) D^r(\epsilon), \quad (2)$$

$$\Pi^r(\omega) = \frac{2}{\pi} \sum_\alpha \int d\epsilon \Gamma_\alpha(\epsilon - \omega - \mu_\alpha) f(\epsilon - \omega - \mu_\alpha) G^r(\epsilon). \quad (3)$$

The NCA expressions for the lesser self-energy of the pseudofermion, $G^<(\omega) = \Sigma^<(\omega)|G^r(\omega)|^2$, and slave-boson, $D^<(\omega) = \Pi^<(\omega)|D^r(\omega)|^2$, are

$$\Sigma^<(\omega) = \frac{2}{\pi} \sum_\alpha \int d\epsilon \Gamma_\alpha(\omega - \epsilon - \mu_\alpha) f(\omega - \epsilon - \mu_\alpha) D^<(\epsilon), \quad (4)$$

$$\Pi^<(\omega) = \frac{2}{\pi} \sum_\alpha \int d\epsilon \Gamma_\alpha(\epsilon - \omega - \mu_\alpha) f(\omega - \epsilon + \mu_\alpha) G^<(\epsilon). \quad (5)$$

Here, $\Gamma_\alpha(\omega) \equiv \Gamma_\alpha \rho_{c,\alpha}(\omega)$ with $\Gamma_\alpha = \pi|U_\alpha|^2$ with $\rho_{c,\alpha}(\omega) \propto |\omega - \mu_\alpha|$ and $f(\omega) = [1 + e^{\beta\omega}]^{-1}$ is the Fermi function.

The physical spectral function, $\rho(\omega, V)$, is the convolution of pseudofermion and slave-boson Greens function

$$\rho(\omega, V) = \frac{i}{2\pi^2 Z} \int d\epsilon [ImD^r(\epsilon)G^<(\omega + \epsilon) - D^<(\epsilon)ImG^r(\omega + \epsilon)]. \quad (6)$$

The normalization factor $Z = \frac{i}{\pi} \int d\omega [D^<(\omega) - G^<(\omega)]$ enforces the constraint, $\langle Q \rangle = 1$. The current is given by [28]

$$I(V, T) = \frac{2e}{\hbar} \int d\omega \frac{2\Gamma_L(\omega)\Gamma_R(\omega)}{\Gamma_L(\omega) + \Gamma_R(\omega)} \rho(\omega, V, T) \times [f(\omega + eV/2) - f(\omega - eV/2)]. \quad (7)$$

The nonlinear conductance $G(V) = dI(V)/dV$ is computed by numerical derivative of the current $I(V)$, whereas the linear-response conductance is directly obtained from

$$G(0, T) = \frac{2e^2}{\hbar} \int d\omega \frac{2\Gamma_L(\omega)\Gamma_R(\omega)}{\Gamma_L(\omega) + \Gamma_R(\omega)} \left(-\frac{\partial f(\omega)}{\partial \omega} \right) \times \rho(\omega, V = 0). \quad (8)$$

Eqs.(4)-(5) together with the Dyson equation for $G(\omega)$ and $D(\omega)$ forms a self-consistent set of integral equations. These equations are iterated until a solution is found with which Eqs.(6)-(8) can be evaluated.

Results. We now turn to a discussion of the self-consistent solution of Eqs. (2)-(5); the results are summarized in the phase diagram Fig. 1(a). For simplicity, we focus on the particularly simple case with parity (left-right) symmetry, $U_L = U_R$, $\Gamma_L = \Gamma_R \equiv \frac{\Gamma}{2}$.

For larger values of $j = \Gamma, |\mu|$ (or $j - j^* > 0.1D$) with $\Gamma^* \sim 0.05D$ and $\mu^* \sim -0.05D$ being crossover scales at a fixed temperature $T_0 \sim 10^{-7}D$, our results show clear 2CK behaviors at low temperatures $T < T_K$ where T_K is the Kondo temperature defined as the temperature where $G(0, T)$ deviates from a $\sim \sqrt{T}$ behavior[27], in agreement with its conventional definition: $G(0, T_K) = G(0, 0)/2$.

However, for smaller values of j with $j - j^* < 0.1D$, we find universal power-law scaling of $G(T, 0)$ distinct from both 2CK (*i.e.* $\sim \sqrt{T}$) and one-channel Kondo (*i.e.* $\sim T^2$) [29] behavior at temperatures $T \gg T^*$ where T^* is the crossover energy scale, describing the 2CK-LM crossover. Note that the NCA gives reliable results for $I(V, T)$ even in the single-channel Kondo case as long as $T \gtrsim 0.1T_K$.

The crossover scale is finite for any non-vanishing gate-voltage ($\mu \neq 0$). We checked that the crossover scales $\Gamma^*, |\mu^*|$ vanish as $T \rightarrow 0$ in a power-law fashion, consistent with the general expectation that Kondo screening in graphene can be induced by arbitrarily small doping ($\mu \neq 0$).

The local density of states $\rho(\omega, V)$, given by Eq.(6), is shown in Fig.2. The Kondo peaks occur at the chemical potential μ , and the Kondo temperature T_K follows the pseudogap Kondo behavior with $r = 1$: $T_K \sim$

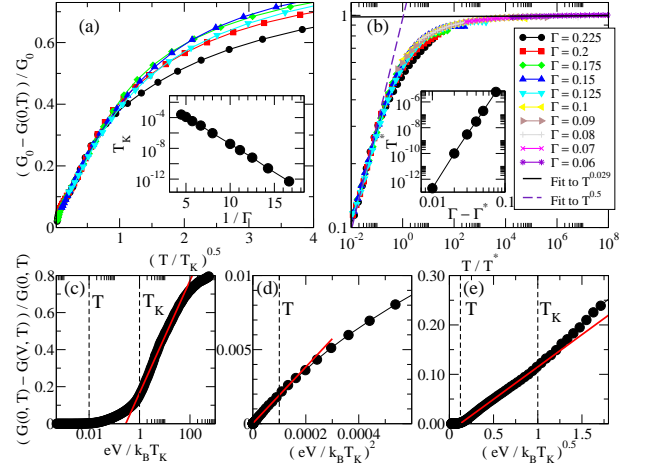


FIG. 3: (a) $(G_0 - G(0, T))/G_0$ calculated from Eq.(8) displays $T^{1/2}$ behavior for $T < T_K$. $G_0 \equiv G(0, T_0)_{\Gamma=0.225D}$ is the linear conductance at the lowest numerically accessible temperature $T_0 \approx 5 \times 10^{-7}D$ at $\Gamma = 0.225D$. Inset: Exponential behavior for $T_K \sim De^{-\pi|\epsilon_d|/\Gamma}$. (b) An additional power law behavior at high temperature for small $\Gamma \approx \Gamma^* \approx 0.05D$, where the crossover scale T^* shows a power law behavior $T^* \sim |\Gamma - \Gamma^*|^{1/\nu}$ with $\nu \sim 0.1$ (Inset). Here, $\epsilon_d = -0.2D$, $\mu = -0.1D$. (c) \sim (e): Non-linear conductance at a large $\Gamma = 0.2D$, and fixed parameters: $T_0 = 5 \times 10^{-7}D$, $\mu = -0.1D$, $\epsilon_d = -0.2D$. The $G(V, T)$ curve shows 2CK Kondo behavior: (c) $\log V$ dependence around $V \sim T_K$ with $T_K \approx 5 \times 10^{-5}D$ and $T = T_0$. (d) V^2 behavior for $V < T$. (e) $T^{1/2}$ 2CK behavior for $T < V < T_K$. Here, the red lines are fits to the corresponding power-law or logarithmic behaviors in different bias regime.

$|\mu| \times e^{(-a/|\mu|)}$ (Inset in Fig.2) where a has the unit of energy and is a function of the bandwidth D and the Kondo coupling J [13]. The $|\omega|$ decay in the vicinity of $\omega = 0$ is a reflection of the Dirac point of the conduction electrons with DOS $\rho_c(\omega) \sim |\omega|$. Comparable results have also been discussed in Refs. [11, 30–33].

Figs. 3(a) and 3(b) shows the linear response conductance $G(0, T)$ obtained via numerical derivative of Eqs. (7) and (8). As long as $\mu \neq 0$, we find clear 2CK behavior at low temperature regime (Fig. 3(a)), with $G(0, T)$ displaying a $T^{1/2}$ behavior for each coupling Γ [27]. The Kondo temperature T_K , behaves as: $T_K \sim De^{-\pi|\epsilon_d|/\Gamma}$ (Fig. 3(a) Inset). For higher temperatures (Fig. 3(b)), we find a universal power-law behavior in T/T^* for $T > T^*$ near $\Gamma^* \approx 0.05D$: $G(0, T) \propto (T/T^*)^\alpha$ with $\alpha \approx 0.029$, indicating the universal crossover from 2CK to LM regime. The crossover energy scale T^* shows a power-law dependence, $T^* \sim |\Gamma - \Gamma^*|^{1/\nu}$ (Fig. 3(b) Inset), where $\nu \sim 0.1$.

$G(V, T)$ at larger Γ shows clear 2CK behavior (see Fig. 3(c)-(e) for $\Gamma = 0.2D$). Fig. 3(c) indicates the $\log V$ behavior predicted for Kondo scattering processes. The V^2 behavior at $V < T$ and $V^{1/2}$ behavior at $T < V < T_K$ in Fig. 3(d) and (e), respectively, are the characteristics

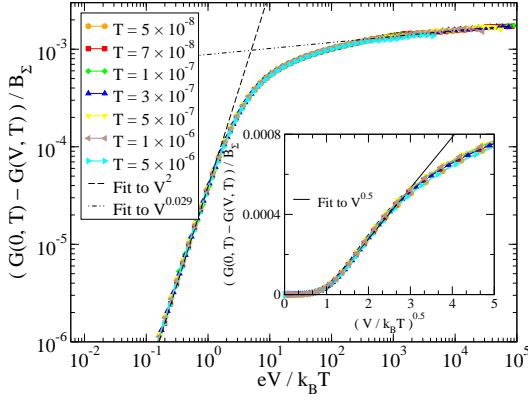


FIG. 4: Temperature scaling of the nonlinear conductance $G(V, T)$ in the universal crossover region with $\Gamma = 0.07D$ and $\mu = -0.08D$ ($\epsilon_d = -0.2D$). All curves collapse onto a universal scaling function. It displays $V^{1/2}$ behavior at $T < V < 10T$ (Inset). For large V (in units of D), $V/T > 10^2$, $G(V, T)$ shows a power law behavior similar to Fig.3(d).

of 2CK physics.

To illustrate the crossover between the 2CK and LM regimes, $G(V, T)$ is shown in Fig. 4 and Fig. 5. Fig. 4, demonstrates V/T scaling [34] of $G(V, T)$ for $\Gamma = 0.07D$ and $\mu = -0.08D$. The resulting curves collapse onto a universal function. For $V/T > 10^2$, $G(V, T)$ shows a power law behavior similar to the one shown in Fig. 3(b); for $1 < V/T < 10$, the behavior follows the 2CK $V^{1/2}$ behavior as shown in the inset of Fig. 4; for $V \ll T$, it shows V^2 Fermi-liquid behavior. Fig. 5(a) is the 2CK scaling plot for large Γ , where all curves follow the scaling function [27], $G(0, T) - G(V, T) = B_\Sigma T^{1/2} H(A \frac{eV}{T_K})$. Here, $H(x) \propto x^{1/2}$ is a universal function and B_Σ and A are non-universal constants [27]. For $V > V^*$, $G(V, T)$ shows the same universal 2CK-LM power-law crossover behavior for small coupling $\Gamma \approx \Gamma^*$ as shown in the linear conductance, $G(0, T)$: $G(0, T) - G(V, T) \propto (V/V^*)^\alpha$ with $\alpha \approx 0.029$, (see Fig. 5(b)). The crossover energy scale V^* also displays a power law behavior $V^* \sim |\Gamma - \Gamma^*|^{1/\nu}$, where $\nu \sim 0.1$, in line with the equilibrium behavior.

Discussions and Conclusions. To make contact with a recent STM experiment [12], it is necessary to generalize our setup to the case where one of the leads is made up of a simple (i.e. one-channel) metal with constant DOS ρ_{tip} near its Fermi energy. The ground state in this case will be that of a Fermi liquid. If, however, the tip is coupled only very weakly ($\Gamma_{tip}/D \ll 1$) to the magnetic adatom on graphene, the corresponding energy scale will be vanishingly small. In this case it is permissible to replace the normal metal lead by a two-channel lead (with constant DOS at the Fermi energy), as the RG equations for the one-channel and two-channel Kondo problem coincide in lowest order. The behavior of $G(V, T)$ in this case are compatible with the results discussed above, see Figs. 1 and 2 of Ref. [24]. Our results, see *e.g.* Fig. 3(c)-(e), are

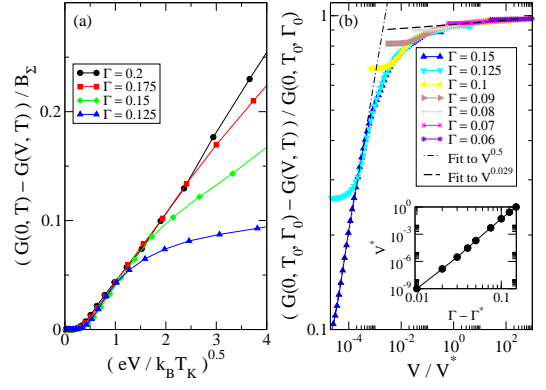


FIG. 5: (a) Scaling of $G(V, T)$ for large Γ (parameters are the same as in Fig.2). For $V < T_K$, $G(V, T)$ collapses onto a single curve $\sim T^{1/2}$. (b) Power law behavior of $G(V, T)$ for $V > V^*$. Here, $G(0, T_0, \Gamma_0)$ refers to the linear conductance at a fixed temperature $T_0 = 5 \times 10^{-7}D$ and a fixed coupling $\Gamma_0 = 0.2D$. Inset: Power law behavior of the crossover energy scale $V^* \sim |\Gamma - \Gamma^*|^\alpha$ (see text). Here, $\epsilon_d = -0.2D$, $\mu = -0.1D$.

thus in line with the experimental findings reported in Ref. [12]. Fano-lineshapes, derived from our results are shown in [24].

Universal out-of-equilibrium scaling is currently pursued in a wide range of condensed matter systems. As demonstrated, magnetic adatoms on graphene offer the possibility to study steady state properties in a universal crossover regime. Here, we have addressed the universal crossover regime that separates the local moment regime from the two-channel Kondo regime of adatoms in graphene. Our analysis is based on the two-channel Anderson model in graphene. In particular, we calculated the differential conductance both in the linear and nonlinear regime. For sufficiently large hybridization, we found clear two-channel Kondo signatures. As the hybridization is reduced, the crossover region separating two-channel Kondo and local moment ground states is entered and the crossover is monitored by the narrowing of the Kondo resonances. In the crossover regime, the conductance shows universal power-law behavior. Our results not only agree well a recent scanning tunneling spectroscopy experiment but also provide a comprehensive theoretical analysis of the transport properties of 2CK impurities in graphene.

We thank T. Chowdhury, K. Ingersent, J. Kroha, K. Sengupta, P. Ribeiro, F. Zamani, M. Vojta and in particular H. Manoharan for useful discussions. C.H. C. acknowledges the NSC grant No.98-2112-M-009-010-MY3, No.101-2628-M-009-001-MY3, the NCTS, the MOE-ATU program of Taiwan R.O.C.

[1] A.C. Hewson, The Kondo Problem to Heavy Fermions (Cambridge University Press, Cambridge, UK, 1997).

- [2] P. Nozieres, A. Blandin, J. Phys. (Paris) **41**, 193 (1980).
- [3] N. Andrei and C. Destri, Phys. Rev. Lett. **52**, 364 (1984), P. B. Wiegmann and A. M. Tsvelik, Z. Phys. B **54**, 201 (1985).
- [4] I. Affleck and A. W. W. Ludwig, Nucl. Phys. B **352**, 849 (1991); *ibid.* **360**, 641 (1991). A.W.W. Ludwig, I. Affleck, Phys. Rev. Lett. **67**, 3160 (1991), E. Sela, A.K. Mitchell, L. Fritz, Phys. Rev. Lett. **106**, 147202 (2011).
- [5] V.J. Emery, S. Kivelson, Phys. Rev. B **46**, 10812 (1992); M. Fabrizio, A.O. Gogolin, Phys. Rev. B **51**, 17827 (1995).
- [6] A. K. Mitchell, E. Sela, D. E. Logan, Phys. Rev. Lett. **108**, 086405 (2012).
- [7] R.M. Potok, I.G. Rau, H. Shtrikman, Y. Oreg, and Goldhaber-Gordon, Nature London **446**, 167 (2007).
- [8] D. L. Cox and A. Zawadowski, Adv. Phys. **47**, 599 (1998).
- [9] T. Chichorek *et al.*, Phys. Rev. Lett. **94**, 236603 (2005).
- [10] K. Sengupta and G. Baskaran, Phys. Rev. B **77**, 045417 (2008).
- [11] Matthias Vojta, Lars Fritz and Ralf Bulla, Europ. Phys. Lett. **90**, 27006 (2010).
- [12] L. S. Mattos *et al.*, (un-published); L.S. Mattos, “Correlated electrons probed by scanning tunneling microscopy”, PhD. thesis, Stanford University (2009).
- [13] David Withoff and Eduardo Fradkin, Phys. Rev. Lett. **64**, 1835 (1990).
- [14] C. Gonzalez-Buxton and K. Ingersent, Phys. Rev. B **57**, 14254 (1998).
- [15] K. Ingersent and Q. Si, Phys. Rev. Lett. **89**, 076403 (2002).
- [16] Matthew Glossop *et al.*, Phys. Rev. Lett. **107**, 076404 (2011).
- [17] Lars Fritz and Matthias Vojta, Phys. Rev. B **70**, 214427 (2004).
- [18] F. Zamani, T. Chowdhury, P. Ribeiro, K. Ingersent, and S. Kirchner, *pss* in print (2013) and arXiv:1211.4450.
- [19] F. Zamani *et al.*, in preparation (2013).
- [20] I. Schneider, L. Fritz, F. B. Anders, A. Benlagra, M. Vojta, Phys. Rev. B **84**, 125139 (2011).
- [21] Luca Dell’Anna, J. Stat. Mech. P01007 (2010).
- [22] Zhen-Gang Zhu, Kai-He Ding, and Jamal Berakdar, Eur. Phys. Lett. **90**, 67001 (2010).
- [23] T. O. Wehling *et al.*, Phys. Rev. B. **81** 085413 (2010).
- [24] see additional supplemental material.
- [25] D. L. Cox and A. L. Ruckenstein, Phys. Rev. Lett. **71**, 1613 (1993).
- [26] Ned S. Wingreen and Y. Meir, Phys. Rev. B **49**, 11040 (1994).
- [27] Matthias H. Hettler, Johann Kroha, and Selman Hershfield, Phys. Rev. Lett. **73**, 1967 (1994); Ch. Kolf, J. Kroha, M. Ternes, and W.-D. Schneider, Phys. Rev. Lett. **58**, 5649 (1998).
- [28] Y. Meir and Ned S. Wingreen, Phys. Rev. Lett. **68**, 2512 (1992).
- [29] M. Grobis, I. G. Rau, R. M. Potok, H. Shtrikman, and D. Goldhaber-Gordon, Phys. Rev. Lett. **100**, 246601 (2008).
- [30] P. S. Cornaglia, Gonzalo Usaj, C. A. Balseiro, Phys. Rev. Lett. **102**, 046801 (2009).
- [31] Huai-Bin Zhuang *et al.* Eur. Phys. Lett. **86**, 58004
- [32] Ahen Gang Zhu and Jamal Berakdar, Phys. Rev. B **84**, 165105 (2011).
- [33] Lin Li *et al.*, arXiv:1204.2696v1 (2012).
- [34] S. Kirchner and Q. Si, Phys. Rev. Lett. **103**, 206401 (2009).